

Dynamical current correlation functions of simple classical liquids for intermediate wave numbers

W. Götze and M. Lücke

Physik-Department der Technischen Universität and Max-Planck-Institut für Physik, München, Germany

(Received 7 May 1974; revised manuscript received 23 December 1974)

The longitudinal and transversal current-current correlation functions of simple classical liquids are expressed in terms of restoring forces and frequency-dependent relaxation kernels within the framework of Mori's theory. The spectra of the relaxation kernels are approximated by the decay of one-mode excitation into pairs of two longitudinal modes and into pairs of one longitudinal and one transversal mode. The decay vertex is given by an irreducible three-particle distribution function which is approximately expressed in terms of two-particle distribution functions taking three-particle hard-core correlations into account. The resulting nonlinear integral equations are solved by iteration for liquid argon parameters and the obtained current excitation spectra are compared with the curves found by computer simulations and by neutron scattering experiments.

I. INTRODUCTION

Liquid argon is an example of a simple classical fluid whose excitation spectrum has been studied extensively during the past years. By inelastic-neutron-scattering experiments^{1,2} the spectrum of density fluctuations as a function of the excitation wave number has been measured. Beginning with the pioneering work of Rahman,^{3,4} computer experiments have been performed^{5,6} yielding the excitation spectrum for longitudinal modes in quantitative agreement with the scattering data; the excitation spectrum for transverse modes has also been determined. In this paper we want to develop a microscopic theory for the abovementioned data.

The current-current correlation functions

$$\chi_{\alpha\beta}(\vec{q}, z) = -\langle j_{\alpha}^*(\vec{q}); j_{\beta}(\vec{q}) \rangle_z,$$

depending on wave vector \vec{q} and frequency z , are the appropriate mathematical quantities for describing the excitations in fluids. Here α, β denote Cartesian components of the particle current $\vec{j}(\vec{q})$. Rotational symmetry of simple liquids implies that there are only two independent quantities: the longitudinal susceptibility $\chi_L(q, z)$ and its transverse counterpart $\chi_T(q, z)$. Whereas $\chi_L(q, z)$ describes fluctuations of density and longitudinal current, $\chi_T(q, z)$ describes shear motion. They depend on the modulus $q = |\vec{q}|$ of the wave vector only:

$$\begin{aligned} \chi_{\alpha\beta}(\vec{q}, z) &= (q_{\alpha}q_{\beta}/q^2)\chi_L(q, z) \\ &+ (\delta_{\alpha\beta} - q_{\alpha}q_{\beta}/q^2)\chi_T(q, z). \end{aligned} \quad (1)$$

In the following it is more convenient to work with Kubo's relaxation function $\Phi(z) = [\chi(z) - \chi(z=0)]/z$ instead of with the susceptibility $\chi(z)$.

Since $\chi(z)$ as well as $\Phi(z)$ are holomorphic functions $F(z)$ for nonreal frequencies decreasing sufficiently fast for large values of z they allow for a

spectral representation

$$F(z) = \int d(\omega/\pi) F''(\omega)/(\omega - z). \quad (2a)$$

The spectral function $F''(\omega)$ is the discontinuity of $F(z)$ across the real axis,

$$F(\omega \pm i0) = F'(\omega) \pm iF''(\omega). \quad (2b)$$

The spectral functions for the currents $\Phi_{L,T}''(q, \omega)$ are real, non-negative, and even in ω ; they characterize the longitudinal or transverse excitation spectrum of the system. If $\Phi''(q, \omega)$ is large excitations with wave number q and frequency ω can be created easily whereas smallness of $\Phi''(q, \omega)$ means that there are no excitation states accessible. Peaks of $\Phi''(q, \omega)$ at positions $\omega_{\max}(q)$ in the ω - q half-plane represent propagating modes with dispersion $\omega_{\max}(q)$ in the fluid, their lifetime being given by the inverse of the width of the resonance. The continuity equation connects the longitudinal current function $\Phi_L''(q, \omega)$ with the density relaxation function $\Phi_{\rho\rho}''(q, \omega)$ by

$$\Phi_{\rho\rho}''(q, \omega) = (q/\omega)^2 \Phi_L''(q, \omega). \quad (3)$$

The coherent-scattering cross section for neutrons with energy loss ω and momentum transfer q is proportional to van Hove's correlation function⁷ $S(q, \omega)$. The generalized fluctuation dissipation theorem⁸

$$\int dt e^{i\omega t} \langle A^*(t)B \rangle = -2(1 - e^{-\omega/T})^{-1} \langle A^*; B \rangle''_{\omega} \quad (4a)$$

simplifies for classical systems to

$$\int dt e^{i\omega t} \langle A^*(t)B \rangle = 2T \Phi_{AB}''(\omega) \quad (4b)$$

and thus it relates $S(q, \omega)$ to $\Phi_{\rho\rho}''(q, \omega)$ by

$$S(q, \omega) = 2T\Phi''_{\rho\rho}(q, \omega) \quad (5)$$

(T denotes the temperature, units are chosen such that Boltzmann's constant k_B and \hbar equal unity). In the following we will develop a theory for $\Phi''_{L,T}(q, \omega)$ for values of q between 0.5 and 4 Å⁻¹; these wave numbers are large enough not to be in the regime of hydrodynamic motion and they are small enough not to be in a regime of gas behavior; it is the regime covered by neutron scattering experiments and by computer simulations.³⁻⁶

Provided there exist $2N$ moments of the spectral function

$$c_n = \int d(\omega/\pi) \omega^n \Phi''(\omega), \quad n=0, 1, \dots, 2N \quad (6a)$$

the following high-frequency asymptotic series can be written for $\Phi(z)$:

$$\Phi(z) = -\frac{1}{z} \sum_{n=0}^{N-1} c_{2n} z^{-2n} + \Phi_N(z) z^{-2N}. \quad (6b)$$

Here $\Phi(z)$ stands for $\Phi_{L,T}(q, z)$ or $\Phi_{\rho\rho}(q, z)$ and $\Phi_N(z)$ is a Cauchy integral of type (2a) with the spectral function $\Phi''_N(\omega) = \omega^{2N} \Phi''(\omega)$. Note that the odd moments c_{2n+1} vanish. Since $\Phi''(\omega)$ is non-negative it is well known⁹ that one can write $\Phi(z)$ as a continued fraction,

$$\Phi(z) = \frac{-a_0^2}{z - \frac{a_1^2}{z - \frac{a_2^2}{z - \dots - \frac{a_{N-1}^2}{z + G_N(z)}}}} \quad (7a)$$

where $G_N(z)$ is some Cauchy integral of type (2a). There is an algorithm⁹ expressing the real numbers a_0, \dots, a_{N-1} by the first $2N$ moments, e.g.,

$$\begin{aligned} a_0^2 &= c_0, \\ a_1^2 &= c_2/c_0, \\ a_2^2 &= (c_4/c_2) - (c_2/c_0). \end{aligned} \quad (7b)$$

The representation of correlation functions as continued fraction (7) has two important advantages. First, while the series (6b) diverges in the frequency regime of interest the continued fraction (7a) converges uniformly off the real axis, provided there are no high-frequency pathologies for $\Phi(z)$. Hence reasonable approximations for $G_N(z)$ by smooth functions may bring out a good approximation for the resonance structure of $\Phi(z)$ in the complete frequency range. Second, whatever approximation is made for $G_N(z)$, $\Phi(z)$ will have the correct first $2N$ moments c_n . The even moments of $\Phi''_{AA}(\omega)$ are given¹⁰ as static susceptibilities of the n th time derivatives $A^{(n)} = (-i\partial_t)^n A$,

$$c_{2n} = \int d(\omega/\pi) \omega^{2n} \Phi''_{AA}(\omega) = -\langle A^{(*)^{(n)}}; A^{(n)} \rangle_{z=0}, \quad (8a)$$

and since static susceptibilities correspond classically to equal time correlations one finds

$$c_{2n} = \langle A^{(*)^{(n)}} A^{(n)} \rangle / T. \quad (8b)$$

The zeroth moment of the current relaxation functions in simple liquids yields the q -independent number n/m , where n is the average particle density and m is the particle mass:

$$\int d(\omega/\pi) \Phi''_{L,T}(q, \omega) = n/m. \quad (9)$$

For the longitudinal case (9) holds also quantum mechanically, expressing the well known f -sum rule.

The second moment can be calculated¹¹ directly for a system of particles interacting by a two-body potential $v(r)$:

$$\int d(\omega/\pi) \omega^2 \Phi''_{\alpha\beta}(\vec{q}, \omega) = \Omega_{\alpha\beta}^2(\vec{q}) n/m, \quad (10a)$$

where the frequency squares $\Omega_{\alpha\beta}^2(\vec{q})$ denote

$$\begin{aligned} \Omega_{\alpha\beta}^2(\vec{q}) &= \Omega_{\alpha\beta}^2(\vec{q})|_{\text{kin}} + \Omega_{\alpha\beta}^2(\vec{q})|_{\text{pot}}, \\ \Omega_{\alpha\beta}^2(\vec{q})|_{\text{kin}} &= q^2 v_{\text{th}}^2 [3q_\alpha q_\beta / q^2 + (\delta_{\alpha\beta} - q_\alpha q_\beta / q^2)], \\ \Omega_{\alpha\beta}^2(\vec{q})|_{\text{pot}} &= (n/m) \int d\vec{r} (1 - e^{-i\vec{q} \cdot \vec{r}}) g(r) \nabla_\alpha \nabla_\beta v(r). \end{aligned} \quad (10b)$$

Here $v_{\text{th}} = (T/m)^{1/2}$ is the thermal velocity and $g(r)$ is the pair-correlation function giving the probability of finding two particles in a distance r .

In analogy with Eq. (1) the matrix $\Omega_{\alpha\beta}^2(\vec{q})$ is given by two independent functions, $\Omega_L^2(q)$ and $\Omega_T^2(q)$. Because of Eq. (6b) these $\Omega_{L,T}^2(q)$ have the physical meaning of high-frequency restoring forces of the fluid. They have been related to generalized elastic moduli.¹²⁻¹⁴ For small wave numbers $\Omega_{L,T}(q)$ are linear functions of q and $\Omega_L(q)/\Omega_T(q) \rightarrow \sqrt{3}$. Since the pair-correlation function $g(r)$ has a peak at the nearest-neighbor distance, $\Omega_L(q)$ shows a characteristic minimum at the corresponding wave vector. On the other hand, $\Omega_T(q)$ is rather flat in the mentioned regime of q values exhibiting only faint oscillations.

Substituting the moments (9) and (10) into Eqs. (7) one gets for the transverse current relaxation function the expression

$$\Phi_T(q, z) = \frac{(-n/m)[z + M_T(q, z)]}{z^2 - \Omega_T^2(q) + z M_T(q, z)}. \quad (11)$$

Here we have written $G_2 = M_T(q, z)$. The mathematical structure of (11) is analogous to the relaxation function describing a Brownian particle

moving in an oscillator potential with characteristic frequency $\Omega_T(q)$ and in a field of fluctuating forces whose spectrum is given by $M_T''(q, \omega)$.

It would not be very helpful to write down the analog of Eq. (11) for the longitudinal current relaxation function since this representation would not automatically contain the conservation law (3). Therefore let us perform the continued fraction (7a) for $\Phi_{\rho\rho}(q, z)$. Equations (9) and (10) then yield the second and fourth moment while the zeroth moment according to Eqs. (8a) and (8b) reads

$$\int d(\omega/\pi) \Phi_{\rho\rho}''(q, \omega) = \chi_{\rho\rho}(q, z=0) = ns(q)/T, \quad (12a)$$

where $s(q)$ is the structure factor of the classical liquid,

$$s(q) = 1 + n \int d\vec{r} e^{i\vec{q} \cdot \vec{r}} [g(r) - 1]. \quad (12b)$$

Hence one gets

$$\Phi_{\rho\rho}(q, z) = [-nq^2/m\Omega_0^2(q)] \frac{1}{z - \frac{\Omega_0^2(q)}{z - \frac{\Delta^2(q)}{z + M_L(q, z)}}}. \quad (13)$$

Here we have introduced the abbreviations

$$\Omega_0^2(q) = nq^2/m\chi_{\rho\rho}(q, z=0) = q^2T/m s(q), \quad (14a)$$

$$\Delta^2(q) = \Omega_L^2(q) - \Omega_0^2(q), \quad (14b)$$

and have written in Eq. (7a) $G_4(z) = M_L(q, z)$. The quantity $\Omega_0^2(q)$ is a restoring force of the fluid for zero-frequency compressions. For small wave numbers $\Omega_0(q) = qc$, where c is the isothermal sound velocity. Similar to $\Omega_L(q)$, $\Omega_0(q)$ also shows a pronounced minimum at the reciprocal interparticle distance. Note that $\Delta^2(q)$ is positive because of the Cauchy-Schwarz inequality relating the first three moments of $\Phi_{\rho\rho}''(q, \omega)$. From Eqs. (3), (12a), and (14a) one gets

$$(z/q)^2 \Phi_{\rho\rho}(q, z) = \Phi_L(q, z) + zn/m\Omega_0^2(q),$$

and hence Eq. (13) can be rewritten in a form which guarantees the correct structure factor,

$$\Phi_L(q, z) = \frac{(-zn/m)[z + M_L(q, z)]}{z[z^2 - \Omega_L^2(q)] + [z^2 - \Omega_0^2(q)]M_L(q, z)}. \quad (15)$$

This function indicates that the longitudinal motion is characterized by two oscillator frequencies $\Omega_L(q)$ and $\Omega_0(q)$ and a fluctuating force which switches from one resonance to the other. The spectrum of the fluctuating force is given by $M_L''(q, \omega)$. The problem of the following theory is

evaluating the kernels $M_L, \tau(q, z)$.

Expressing the response functions Φ by some kernel $G_N(z)$ is common to most of the previous theories. The Vlasov-equation result or mean-field approximation for $\Phi_{\rho\rho}$ can be obtained, e.g., by replacing Δ and M_L in Eq. (3) by the free-gas values. After this approximation was proved to be unsatisfactory¹⁵ Kerr's suggestion¹⁶ to modify this approach by a replacement of the free-gas autocorrelation function by the correct one of the liquid was followed by Singwi *et al.*¹⁷ Pathak and Singwi replaced the autocorrelation function by a Gaussian whose width was fixed by the fourth sum rule of $\Phi_{\rho\rho}$ and determined the polarization potential via the structure function. The good results of this work and of Kugler,¹⁸ who introduces a frequency-dependent Gaussian polarization potential, served as justification of the approximations. Similar in spirit is the approximation of Hubbard and Beeby,¹⁹ who start from the phonon picture of crystals.

Obviously, Eqs. (11) and (15) reduce to the exact hydrodynamic relaxation functions of Kadanoff and Martin²⁰ if q and z approach zero. $M_T(q, z)$ is the kernel of the generalized transport coefficient $D(q, z)$,

$$iD(q, z) = -\frac{\Omega_T^2(q)/q^2}{z + M_T(q, z)}. \quad (16a)$$

In the hydrodynamic limit it is related to the shear viscosity η by $D(0, 0) = \eta/nm$. Similarly, $M_L(q, z)$ is the kernel of the transport coefficient $\Gamma(q, z)$,

$$i\Gamma(q, z) = -\frac{\Delta^2(q)/q^2}{z + M_L(q, z)}, \quad (16b)$$

which, in the hydrodynamic limit, determines the sound damping constant $\Gamma(0, 0) = (\zeta + 4\eta/3)/nm$. Equation (16b) results from a comparison with the corresponding hydrodynamic expression²⁰ with an additional neglect of heat diffusion. Several phenomenological models for $D(q, z)$ and $\Gamma(q, z)$ have been discussed^{4, 21, 6} since Chung and Yip²² started generalized hydrodynamics approximations. They proposed Lorentzians for the generalized transport coefficients, interpolating the wave-vector-dependent relaxation rates between the hydrodynamic and the free-gas limit. In this way a good fit of the experimental data^{3, 4} was obtained. The fit could be improved by Ailawadi *et al.*⁴ by assuming Gaussian time behavior of Γ and D . Levesque *et al.*⁶ also concluded from their very accurate data that for wave vectors around 1 \AA^{-1} Lorentzians are not an adequate enough description. For long wavelengths it has been found⁶ that a long time tail appears in the generalized viscosity such that $D(q, z)$ is best described by the sum of two Lorentzians.

Mori²³ has developed systematically the formal technique of expressing correlation functions by continued fractions like the one in Eq. (7a). Extending the projector formalism of Zwanzig²⁴ he related the kernels $G_N(z)$ to certain reduced matrix elements of the Liouville operator of the system. Using phenomenological models²⁵ for these kernels similar to the ones discussed above it was also possible²⁶ to describe the experimental excitation spectrum. The mentioned theoretical treatments demonstrated²⁷ that the framework presented by Eqs. (11) and (15) is adequate to describe the spectrum of liquids. On the other hand it is obvious that in the mentioned papers no complete microscopic theory for the response functions has been given, since the spectra for the fluctuating forces have been put into the formulas more or less as fit parameters.

Lebowitz *et al.* and Forster and Martin²⁸ started systematic attempts²⁹ to derive kinetic equations for denser fluids where the Boltzmann equation does no longer hold. At present it cannot be seen, however, whether this approach can be applied to the real densities of liquids. One can generalize in a formally exact way kinetic equations similarly as one does for the hydrodynamic equations. The problem then consists of solving the corresponding integral equations and of finding approximations for the integral kernels. With the ansatz that the kernels are Lorentzian and a fit of the relevant rates to the hydrodynamic limit Duderstadt and Akcasu and Jhon and Forster³⁰ could achieve good agreement of the calculations with the data for argon.

In the following a microscopic theory for the kernels is presented. Starting with Mori's expression²³ for $M_L(q, z)$ and $M_T(q, z)$ the spectra of the fluctuating forces are expressed approximately in terms of two-mode decay integrals (Sec. II). In this way $M_{L,T}$ are represented in terms of the correlation functions $\Phi_{L,T}$. Besides the structure factor $s(q)$ and the potential $v(r)$ no new unknowns enter the theory. Then (Sec. III) the solution of the nonlinear equations is obtained by iteration and our theoretical curves are compared with experiments. In Sec. IV the results are discussed and a physical interpretation of the main features of the excitation spectrum is given.

II. APPROXIMATION FOR THE FLUCTUATION KERNELS

A. General formulas

Mori's theory²³ starts by introducing the scalar product

$$(A|B) = \chi_{A^*B}(z=0) = \langle A^* B \rangle / T \quad (17)$$

in the linear space of dynamical variables A, B, \dots . The Liouville operator \mathcal{L} acting upon dynamical variables is defined by

$$\mathcal{L}A(t) = -i\partial_t A(t) = i\{H, A(t)\}, \quad (18a)$$

where H is the Hamiltonian of the system and the Poisson bracket reads

$$\{H, A\} = \sum_{\alpha} \left(\frac{\partial H}{\partial q_{\alpha}} \frac{\partial A}{\partial p_{\alpha}} - \frac{\partial H}{\partial p_{\alpha}} \frac{\partial A}{\partial q_{\alpha}} \right). \quad (18b)$$

The generalization of (18a) to quantum-mechanical systems is obviously $\mathcal{L}A(t) = [H, A(t)]$. Since the formal solution of (18a) is

$$A(t) = e^{i\mathcal{L}t} A, \quad (19)$$

with \mathcal{L} being Hermitian one can write Kubo's A - B relaxation function

$$\Phi_{AB}(z) = (\langle\langle A^*; B \rangle\rangle_{z=0} - \langle\langle A^*; B \rangle\rangle_z) / z \quad (20a)$$

as a resolvent matrix element

$$\Phi_{AB} = (A|[\mathcal{L} - z]^{-1}|B). \quad (20b)$$

The spectral function $\Phi''_{AB}(\omega) = \pi(A|\delta(\omega - \mathcal{L})|B)$ in the classical limit is given by the Fourier integral (4b).

The functions introduced in Sec. I are special cases with $A=B$ and A being, respectively, the transverse current $j_T(\vec{q})$, the longitudinal current $j_L(\vec{q})$, or the density $\rho(\vec{q})$. Introducing the one-dimensional projector $\mathcal{P} = |A\rangle\langle A| / (A|A)$ and its complement $\mathcal{Q} = 1 - \mathcal{P}$, one can write²³ the resolvent in the standard fashion,

$$\Phi_{AA}(z) = -a^2 / [z - b + m(z)], \quad (21a)$$

where $a^2 = (A|A)$, $b = (A|\mathcal{L}|A)/a^2$, and $m(z)$ is the reduced resolvent matrix element

$$m(z) = (\mathcal{Q}\mathcal{L}A|[\mathcal{Q}\mathcal{L}\mathcal{Q} - z]^{-1}|\mathcal{Q}\mathcal{L}A)/a^2 \quad (21b)$$

defined in the space orthogonal to $|A\rangle$. In our examples the numbers b vanish.

Iteration of Eqs. (21) yields Mori's continued fraction. Applying Eqs. (21) twice with $A = j_T(\vec{q})$ one gets Eq. (11) with

$$M_T(q, z) = N_T(q, z) / \Omega_T^2(q), \quad (22a)$$

$$N_T(q, z) = (m/n)(\mathcal{L}^2 j_T(\vec{q})|\mathcal{Q}_T^{(1)} \times [\mathcal{Q}_T^{(2)} \mathcal{Q}_T^{(1)} \mathcal{L} \mathcal{Q}_T^{(1)} \mathcal{Q}_T^{(2)} - z]^{-1} \times \mathcal{Q}_T^{(1)}|\mathcal{L}^2 j_T(\vec{q})). \quad (22b)$$

Here we have denoted the projector orthogonal to $j_T(\vec{q})$ by $\mathcal{Q}_T^{(1)}$ and the projector orthogonal to $\mathcal{L}j_T(\vec{q})$ by $\mathcal{Q}_T^{(2)}$. We also used $\mathcal{Q}_T^{(1)}\mathcal{L}j_T(\vec{q}) = \mathcal{L}j_T(\vec{q})$ and $\mathcal{Q}_T^{(2)}\mathcal{L}^2 j_T(\vec{q}) = \mathcal{L}^2 j_T(\vec{q})$; these relations hold since $\mathcal{L}^2 j_T(\vec{q})$ and $j_T(\vec{q})$ have a parity under time inversion opposite to that of $\mathcal{L}j_T(\vec{q})$. This causes also $\mathcal{Q}_T^{(2)}\mathcal{Q}_T^{(1)}\mathcal{L}\mathcal{Q}_T^{(1)}\mathcal{Q}_T^{(2)}$ to be equal to $\mathcal{Q}_T^{(2)}\mathcal{L}\mathcal{Q}_T^{(2)}$. Similar-

ly, applying Eqs. (21) three times with $A = \rho(\vec{q})$ one gets Eq. (15) with

$$M_L(q, z) = N_L(q, z) / \Delta^2(q), \quad (23a)$$

$$N_L(q, z) = (m/n) (\mathcal{L}^2 j_L(\vec{q}) | \mathcal{Q}_L^{(1)} \\ \times [\mathcal{Q}_L^{(2)} \mathcal{Q}_L^{(1)} \mathcal{L} \mathcal{Q}_L^{(1)} \mathcal{Q}_L^{(2)} - z]^{-1} \\ \times \mathcal{Q}_L^{(1)} | \mathcal{L}^2 j_L(\vec{q})), \quad (23b)$$

where $\mathcal{Q}_L^{(0)}$, $\mathcal{Q}_L^{(1)}$, and $\mathcal{Q}_L^{(2)}$ successively denote the projector respectively orthogonal to $\rho(\vec{q})$, $\mathcal{Q}_L^{(0)} \mathcal{L} \rho(\vec{q}) = -q j_L(\vec{q})$, and $\mathcal{Q}_L^{(1)} \mathcal{Q}_L^{(0)} \mathcal{L} \mathcal{Q}_L^{(0)} \mathcal{L} \rho(\vec{q}) = [\mathcal{L}^2 - \Omega_0^2(q)] \rho(\vec{q})$. One also has to note $\mathcal{Q}_L^{(1)} \mathcal{Q}_L^{(0)} \mathcal{L} \mathcal{Q}_L^{(0)} \mathcal{Q}_L^{(1)} = \mathcal{Q}_L^{(1)} \mathcal{L} \mathcal{Q}_L^{(1)}$ and to make use of the orthogonality of quantities with opposite time-inversion symmetry as explained above. Equations (11), (15), (22), and (23) with the underlying definitions are exact. The problem consists of evaluating the kernels (22) and (23) approximately.

B. Two-mode approximation

It is advantageous to express the quantities $\mathcal{L} j_\alpha(\vec{q})$, $\mathcal{L}^2 j_\alpha(\vec{q})$, etc., by the phase space density

$$f(\vec{p}, \vec{q}) = (2\pi)^3 \sum_n \delta(\vec{p} - \vec{p}_n) e^{-i\vec{q} \cdot \vec{r}_n}.$$

For example the particle density and current den-

$$\mathcal{L}^2 j_\alpha(\vec{q}) = \sum_{\vec{k}} k_\alpha (\vec{k} \vec{q})^2 f(\vec{k}, \vec{q}) / m^3 + \sum_{\vec{k}} j_\beta(\vec{k}) \rho(\vec{q} - \vec{k}) \{ v(k) k_\alpha k_\beta + v(\vec{q} - \vec{k}) [(\vec{q} - \vec{k})_\alpha (\vec{q} + \vec{k})_\beta + \delta_{\alpha\beta} \vec{q} \cdot (\vec{q} - \vec{k})] \} / m. \quad (25b)$$

Obviously the space of dynamical variables is spanned by products of K distributions

$$f(\vec{p}_1, \vec{q}_1) f(\vec{p}_2, \vec{q}_2) \cdots f(\vec{p}_K, \vec{q}_K) \quad (K=1, 2, \dots).$$

The variable $\mathcal{L}^n j(\vec{q})$, for example, consists of a linear combination of products of k particle distribution functions with $k \leq 2n$. Choosing a set of complete functions $H_n(\vec{p})$, e.g., the Hermitian polynomials, one can expand each one-particle observable as a linear combination of the

$$A_n(\vec{q}) = \sum_{\vec{p}} H_n(\vec{p}) f(\vec{p}, \vec{q}).$$

The set of observables $A_{n_1}(\vec{q}_1) A_{n_2}(\vec{q}_2) \cdots A_{n_K}(\vec{q}_K)$ is then complete. $A_n(\vec{q})$ can be called a one-mode excitation of type n with momentum \vec{q} , $A_{n_1}(\vec{q}_1) \times A_{n_2}(\vec{q}_2)$ is a two-mode excitation of type (n_1, n_2) with momentum $\vec{q}_1 + \vec{q}_2$, etc. The simplest modes are the density and the current density (24c) and products of those.

The resolvents entering Eqs. (22) and (23) de-

sity read

$$\rho(\vec{q}) = \sum_{\vec{p}} f(\vec{p}, \vec{q}), \quad (24a)$$

$$j_\alpha(\vec{q}) = \sum_{\vec{p}} (p_\alpha / m) f(\vec{p}, \vec{q})$$

(here and in the following $\sum_{\vec{p}}$ stands for $\int d\vec{p} / (2\pi)^3$ with the normalization volume V chosen as unity). The Hamiltonian

$$H = \sum_n \frac{p_n^2}{2m} + \frac{1}{2} \sum_{n,m} v(|\vec{r}_n - \vec{r}_m|) \quad (24b)$$

has the presentation

$$H = \sum_{\vec{k}} \frac{k^2}{2m} f(\vec{k}, 0) + \frac{1}{2} \sum_{\vec{k}} \rho^*(\vec{k}) v(k) \rho(\vec{k}), \quad (24c)$$

where $v(k)$ is the Fourier transform of the pair potential. Then one finds for $\tau_\alpha(\vec{q}) = \mathcal{L} j_\alpha(\vec{q})$ the formula

$$\tau_\alpha(\vec{q}) = \sum_{\vec{k}} k_\alpha (\vec{q} \vec{k}) f(\vec{k}, \vec{q}) / m^2 \\ + \sum_{\vec{k}} k_\alpha v(k) \rho^*(\vec{k}) \rho(\vec{k} + \vec{q}) / m. \quad (25a)$$

Similarly one gets

scribe the motion in a space orthogonal to the vectors ρ and j_α . Our *first approximation* consists of writing

$$\mathcal{Q}^{(1)} [\mathcal{Q}^{(2)} \mathcal{Q}^{(1)} \mathcal{L} \mathcal{Q}^{(1)} \mathcal{Q}^{(2)} - z] \mathcal{Q}^{(1)} \\ \approx \mathcal{Q}^{(1)} \mathcal{P}_2 [\mathcal{L} - z]^{-1} \mathcal{P}_2 \mathcal{Q}^{(1)}, \quad (26a)$$

where \mathcal{P}_2 is the projector onto the relevant two-mode excitations,

$$\mathcal{P}_2 = \sum_{\alpha\beta\vec{k}\vec{p}} |j_\alpha(\vec{k}) \rho(\vec{q} - \vec{k})| \\ \times [(j\rho | j\rho)^{-1}]_{\vec{k}\vec{p}}^{\alpha\beta} (j_\beta(\vec{p}) \rho(\vec{q} - \vec{p})). \quad (26b)$$

The *second approximation* consists of completely neglecting the interaction between the two modes; i.e., we assume that under time evolution the two-mode excitations do not mix and just evolve as the products of single modes. To get the relevant matrix

$$\Psi_{\vec{k}\vec{p}}^{\alpha\beta}(\vec{q}, z) = (j_\alpha(\vec{k})\rho(\vec{q} - \vec{k})[\mathcal{L} - z]^{-1}j_\beta(\vec{p})\rho(\vec{q} - \vec{p})) \quad (27)$$

one then can factorize in time space according to

$$\langle A^*(t)B^*(t)CD \rangle = \langle A^*(t)C \rangle \langle B^*(t)D \rangle + \langle A^*(t)D \rangle \langle B^*(t)C \rangle \quad (28a)$$

and obtain the relaxation function (20c) by Fourier transforms,

$$\begin{aligned} \Psi_{\vec{k}\vec{p}}^{\alpha\beta}(\vec{q}, \omega)/T &= \delta_{\vec{k}, \vec{p}}^{\alpha\beta}(\vec{q} - \vec{k})^2 \left(\delta_{\alpha\beta} - \frac{k_\alpha k_\beta}{k^2} \right) \int d\epsilon \frac{\Phi_L''(\vec{q} - \vec{k}, \omega - \epsilon) \Phi_T''(\vec{k}, \epsilon)}{(\omega - \epsilon)^2} \\ &+ \delta_{\vec{k}, \vec{p}}^{\alpha\beta}(\vec{q} - \vec{k})^2 \left(\frac{k_\alpha k_\beta}{k^2} \right) \int d\epsilon \frac{\Phi_L''(\vec{q} - \vec{k}, \omega - \epsilon) \Phi_L''(\vec{k}, \epsilon)}{(\omega - \epsilon)^2} \\ &+ \delta_{\vec{q}, \vec{k} + \vec{p}}^{\alpha\beta} k_\alpha p_\beta \int d\epsilon \frac{\Phi_L''(\vec{q} - \vec{k}, \omega - \epsilon) \Phi_L''(\vec{k}, \epsilon)}{\epsilon(\omega - \epsilon)}. \end{aligned} \quad (29)$$

In this way the frequency-dependent part of the kernels $M_{L,T}(q, z)$ has been expressed in terms of the current relaxation functions.

The idea of representing the space of dynamical variables by products of basic modes and approximating self-energies or memory kernels like $M_{L,T}(q, z)$ by the lowest nonvanishing terms has been used before in other theories of many-particle systems. Kawasaki, Kadanoff and Swift, and Wegner used this procedure to calculate transport coefficients near critical points.³¹ This approximation has also been used to determine the nonregular long-time behavior of correlation functions.³² For these problems the two-mode approximation can be justified since it yields the leading contribution to the singularities of interest. In all theories where there is a diagrammatic expansion available approximations of type (29) present the first term to the energy-dependent part of the polarization operator; this holds in particular for the theory of anharmonic phonons in crystals.³³ Since we do not have a small parameter in classical liquids for the ω - q regime of interest, we cannot give a sophisticated mathematical justification of the preceding approximations. We argue that formula (29) is the simplest contribution to the fluctuating forces in a multimode expansion. The Mori formalism combined with multimode expansions is a possible systematic way of formulating the problem in microscopic terms. In this paper we want to examine the simplest approximation which can be set up within this scheme.

Formula (29) is a Golden Rule type of formula describing the decay of current excitations into pairs of such excitations as indicated in Fig. 1. Notice that there are two decay channels for the

$$\begin{aligned} \Phi_{AB, CD}''(\omega) &= (T/\pi) \int d\epsilon [\Phi_{AC}''(\omega - \epsilon) \Phi_{BD}''(\epsilon) \\ &+ \Phi_{AD}''(\omega - \epsilon) \Phi_{BC}''(\epsilon)]. \end{aligned} \quad (28b)$$

Applying this to Eq. (27) and using the continuity equation to express ρ by the longitudinal current one gets

longitudinal and transverse modes; they may decay into a pair of two longitudinal modes ρj_L or into a pair ρj_T consisting of a longitudinal and a transverse mode. Pair excitations of the type $\rho\rho$ or $j_L j_L$ do not contribute to M because they have the wrong time-inversion parity; in particular decays into two transverse modes are not possible.

C. Three-current vertex

To work out the frequency-independent part of the kernels $M_{L,T}(q, z)$ we notice first, that in our factorization approximation,

$$\begin{aligned} (j_\alpha(\vec{k})\rho(\vec{q} - \vec{k})|j_\beta(\vec{p})\rho(\vec{q} - \vec{p})) \\ = \delta_{\alpha\beta} \delta_{\vec{k}, \vec{p}} n s(\vec{q} - \vec{k}) n/m. \end{aligned} \quad (30)$$

So the projector (26b) has a very simple form. We prefer to work with the matrix $N_{\alpha\beta}(\vec{q}, z)$ instead of with the independent parts

$$N_L(q, z) = \sum_{\alpha\beta} N_{\alpha\beta}(\vec{q}, z) q_\alpha q_\beta / q^2$$

or

$$N_T(q, z) = \sum_{\alpha\beta} N_{\alpha\beta}(\vec{q}, z) (\delta_{\alpha\beta} - q_\alpha q_\beta / q^2) / 2.$$

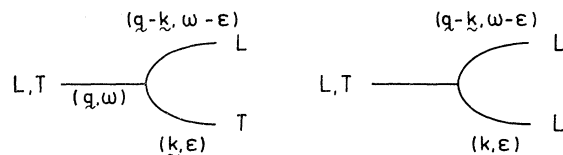


FIG. 1. Decay channels for current excitations into pairs of such modes.

Choosing $\vec{q} = (0, 0, q_3)$ we have $N_L = N_{33}$ and $N_T = (N_{11} + N_{22})/2 = N_{11} = N_{22}$. Substituting Eqs. (26) and (27) into (22) and (23) one gets

$$N_{\alpha\beta}(\vec{q}, z) = \frac{m}{n^3} \sum_{\alpha' \beta' \vec{k} \vec{p}} \varphi_{\alpha'}^{\alpha}(\vec{q}, \vec{k}) \times \Psi_{\vec{k} \vec{p}}^{\alpha' \beta'}(\vec{q}, z) \varphi_{\beta'}^{\beta}(\vec{q}, \vec{p}), \quad (31)$$

where the vertex $\varphi_{\beta}^{\alpha}(\vec{q}, \vec{k})$ is defined by

$$\varphi_{\beta}^{\alpha}(\vec{q}, \vec{k}) = \frac{(\mathcal{L}^2 j_{\alpha}(\vec{q}) | \mathcal{Q}^{(1)} | j_{\beta}(\vec{k}) \rho(\vec{q} - \vec{k}))}{ns(\vec{q} - \vec{k})/m}, \quad (32a)$$

and $\mathcal{Q}^{(1)}$ projects orthogonal to the currents:

$$(\mathcal{L}^2 j_{\alpha}(\vec{q}) | j_{\beta}(\vec{k}) \rho(\vec{q} - \vec{k})) = (n/m)s(\vec{q} - \vec{k})\Omega_{\alpha\beta}^2(\vec{q})|_{\text{kin}} + \int d\vec{r} (1 - e^{-i\vec{q} \cdot \vec{r}}) f_3(\vec{r}, \vec{q} - \vec{k}) \nabla_{\alpha} \nabla_{\beta} v(r)/m^2 + \sum_{\kappa} [\delta_{\alpha\beta} \vec{q} \cdot \vec{k} + 2\kappa_{\alpha} q_{\beta}] v(\kappa) f_3(\vec{k}; \vec{q} - \vec{k})/m^2. \quad (32d)$$

Here

$$f_3(\vec{k}; \vec{q}) = \langle \rho^*(\vec{k}) \rho(\vec{k} - \vec{q}) \rho(\vec{q}) \rangle$$

contains a three-particle correlation function; the occurrence of such a function is not surprising since at the vertex in Fig. 1 three currents interact with each other. One can write

$$f_3(\vec{k}; \vec{q}) = \int d\vec{r} \int d\vec{r}' e^{i\vec{k} \cdot \vec{r} - i\vec{q} \cdot \vec{r}'} \times \{ F_3(\vec{r}; \vec{r}') + n[\delta(\vec{r}) \delta(\vec{r}') + ng(r)\delta(\vec{r}')] + ng(r')\delta(\vec{r}) + ng(r)\delta(\vec{r} - \vec{r}') \}, \quad (33a)$$

where

$$F_3(\vec{r}; \vec{r}') = \sum_{n, m, l} \langle \delta(\vec{r} - \vec{r}_n + \vec{r}_m) \delta(\vec{r}' - \vec{r}_l + \vec{r}_m) \rangle \quad (33b)$$

is the probability to find from a given particle two other particles in distances \vec{r} and \vec{r}' (the prime at the sum indicates that the particles n, m, l are all different). Let us write this function as the uncorrelated probability plus the genuine irreducible three-particle correlation $F(\vec{r}; \vec{r}')$,

$$F_3(\vec{r}; \vec{r}') = n^3 g(r)g(r') + F(\vec{r}, \vec{r}'), \quad (33c)$$

so that

$$f_3(\vec{k}, \vec{q}) = n[1 + ng(\kappa)][1 + ng(q)] + n^2 g(\vec{k} - \vec{q}) + F(\vec{k}; \vec{q}). \quad (33d)$$

After substituting this into Eq. (32d) the first term

$$\mathcal{Q}^{(1)} = 1 - \frac{m}{n} \sum_{\alpha} |j_{\alpha}(\vec{q})| (j_{\alpha}(\vec{q})|$$

The vertex (32a) is the probability amplitude for the decay of one current excitation into two. Since in the classical limit the following identity holds:

$$(j_{\alpha}(\vec{q}) | j_{\beta}(\vec{k}) \rho(\vec{q} - \vec{k})) = \delta_{\alpha\beta} s(\vec{q} - \vec{k})n/m, \quad (32b)$$

one can write

$$\varphi_{\beta}^{\alpha}(\vec{q}, \vec{k}) = \frac{(\mathcal{L}^2 j_{\alpha}(\vec{q}) | j_{\beta}(\vec{k}) \rho(\vec{q} - \vec{k}))}{ns(\vec{q} - \vec{k})/m} - \Omega_{\alpha\beta}^2(\vec{q}). \quad (32c)$$

The scalar product in (32c) evaluated classically yields

of (33d) together with the first term in (32d) yields

$$(n/m)\Omega_{\alpha\beta}^2(\vec{q})s(\vec{q} - \vec{k}),$$

which cancels the last term in Eq. (32c). The second term of (33d), mixing the moments \vec{k} and \vec{q} , yields after insertion into Eq. (32d) the expression

$$(n/m)[\Omega^2(\vec{k}) - \Omega^2(\vec{q} - \vec{k})]|_{\text{pot}}^{\alpha\beta} - i(n/m) \int d\vec{r} e^{i(\vec{k} - \vec{q}) \cdot \vec{r}} g(r) \times [\delta_{\alpha\beta} \vec{q} \cdot \vec{r} + 2q_{\alpha} r_{\beta}] v(r). \quad (33e)$$

This contribution will be neglected; it shows oscillatory behavior vanishing approximately after integrating over \vec{k} . As a result we are left with

$$\varphi_{\beta}^{\alpha}(\vec{q}, \vec{k}) = \int d\vec{r} F(\vec{r}; \vec{q} - \vec{k}) [(1 - e^{-i\vec{q} \cdot \vec{r}}) \nabla_{\alpha} \nabla_{\beta} v(r) - i(\delta_{\alpha\beta} \vec{q} \cdot \vec{r} + 2q_{\alpha} r_{\beta}) v(r)] \times [nms(\vec{q} - \vec{k})]^{-1}. \quad (34)$$

Thus the two-mode approximation (26) of Sec. II B implies that for the fluctuating forces the existence of nontrivial three-particle correlations play an important role: For dilute gases our approximation (34) would imply $M_{L,T} \approx 0$; this is reasonable since in gases the contributions to the damping mechanism are due to two-particle collisions, i.e., due to four current correlations. For systems like solid or liquid argon, on the other hand, which are essentially close-packed hard-core arrangements, the three-particle correlations are crucial and have to play an essential role in

any first-principle theory. Neglecting F in Eq. (33c) one would allow particles n and l in definition (33b) to overlap with their hard core. Since the hard-core volume is a considerable fraction of the total volume available, the approximation $F \sim 0$ would imply considerable errors.

The *third and last approximation* of the present paper consists of taking the hard-core correlations into account approximately by writing

$$F_3(\vec{r}; \vec{r}') \approx n^3 g(r) g(r') \Theta(|\vec{r} - \vec{r}'| - r_1), \quad (35a)$$

i.e.,

$$F(\vec{r}; \vec{r}') = -n^3 g(r) g(r') \Theta(r_1 - |\vec{r} - \vec{r}'|). \quad (35b)$$

Here Θ is the usual step function and r_1 is an appropriate hard-core diameter. In this way the three-current vertex reads

$$\begin{aligned} \varphi_B^\alpha(\vec{q}, \vec{k}) = & - \int d\vec{r}' e^{-i(\vec{q}-\vec{k}) \cdot \vec{r}'} n g(r') \\ & \times G_{\alpha\beta}(\vec{q}, \vec{r}') / s(\vec{q} - \vec{k}), \end{aligned} \quad (36a)$$

with

$$\begin{aligned} G_{\alpha\beta}(\vec{q}, \vec{r}') = & \frac{n}{m} \int d\vec{r} (1 - e^{-i\vec{q} \cdot \vec{r}}) \\ & \times \Theta(r_1 - |\vec{r} - \vec{r}'|) g(r) \nabla_\alpha \nabla_\beta g(r). \end{aligned} \quad (36b)$$

Note that $ng(r')$ in (36a) can be replaced by the Fourier transform of $s(q)$ from Eq. (12b) without changing the result. The second term in (34) is negligible. It involves the product of the pair-correlation function times first derivatives of the potential, but the latter quantities vanish where $g(r)$ is big. The integral (36b) is similar to the one entering $\Omega_{\alpha\beta}^2(\vec{q})$ in Eq. (10b), but here the integration volume is only a sphere of radius r_1 around \vec{r}' . We calculated it for \vec{r}' parallel to \vec{q} and for \vec{r}' perpendicular to \vec{q} , and added the results with the weighting 1 to 2. The product of $g(r)$ times the second potential derivatives is strongly peaked near the interparticle distance. So it is a reasonable approximation¹⁹ to write

$$\begin{aligned} N_L''(q, \omega) = & \frac{Tm\varphi_L^2(q)}{n^3 16\pi^3 q^3} \int_0^\infty dk \int_{|q-k|}^{q+k} d\kappa \int_{-\infty}^\infty d\epsilon \left[\Phi_L''(\kappa, \epsilon) \Phi_T''(k, \omega - \epsilon) \frac{\kappa^3}{\epsilon^2 k} [4k^2 q^2 - (k^2 - \kappa^2 + q^2)^2] \right. \\ & \left. + \Phi_L''(\kappa, \epsilon) \Phi_L''(k, \omega - \epsilon) \kappa^2 \left(\frac{\kappa(k^2 - \kappa^2 + q^2)^2}{k\epsilon^2} - \frac{k[(k^2 - \kappa^2)^2 - q^4]}{\kappa(\omega - \epsilon)} \right) \right], \end{aligned} \quad (39)$$

$$\begin{aligned} N_T''(q, \omega) = & \frac{Tm\varphi_T^2(q)}{n^3 16\pi^3 q^3} \int_0^\infty dk \int_{|q-k|}^{q+k} d\kappa \int_{-\infty}^\infty d\epsilon \left[\Phi_L''(\kappa, \epsilon) \Phi_T''(k, \omega - \epsilon) \frac{\kappa^3}{2\epsilon^2 k} [4k^2 q^2 - (k^2 - \kappa^2 + q^2)^2] \right. \\ & + \Phi_L''(\kappa, \epsilon) \Phi_L''(k, \omega - \epsilon) (\kappa^2/2) \\ & \left. \times [4k^2 q^2 - (k^2 - \kappa^2 + q^2)^2] \left(\frac{\kappa}{k\epsilon^2} - \frac{k}{\kappa(\omega - \epsilon)} \right) \right]. \end{aligned} \quad (40)$$

$$(n/m) g(r) \nabla_\alpha \nabla_\beta v(r) \approx (3\Omega_E^2/4\pi r_0^2) \delta(r - r_0) r_\alpha r_\beta / r^2. \quad (36c)$$

The "Einstein" frequency Ω_E defined by $\Omega_E^2 = (n/3m) \int d\vec{r} g(r) \Delta v(r)$ is known¹² to be particularly sensitive to the hard-core behavior of $v(r)$. The weighted $\bar{G}_{\alpha\beta}(\vec{q}, r_0)$ is taken approximately in front of the integral (36a) thus yielding

$$\varphi_B^\alpha(\vec{q}, \vec{k}) = -\bar{G}_{\alpha\beta}(\vec{q}, r_0). \quad (37a)$$

Notice that the dependence on \vec{k} has dropped out. $\bar{G}_{\alpha\beta}(\vec{q}, r_0)$ is given as usual by two independent functions:

$$\begin{aligned} \bar{G}_{L,T}(q, r_0) = & \Omega_E^2 [f_{L,T}(q, r_0; 1) - f_{L,T}(q, r_0, \tau)] / 4 \\ & + 2\Theta f_{L,T}(q, r_0)(1 - \tau^2)^{1/2}, \end{aligned} \quad (37b)$$

$$f_L(q, r_0; t) = \int_{-t}^t dt' t'^2 (1 - e^{-i\tau_0 t'}) \quad (37c)$$

and $\tau = \cos\Theta = 1 - \frac{1}{2}(r_1/r_0)^2$. For the transverse function $f_T(q, r_0; t)$ one has to replace t'^2 in (37c) by $(1 - t'^2)/2$. As a result we obtained in Eq. (37a) closed expressions for the three current vertices entering Eq. (31) for the kernels $M_{L,T}(q, z)$.

III. CURRENT EXCITATION SPECTRUM

A. Self-consistency equations

Equations (29), (31), and (37) represent the approximations analyzed in this paper. Let us examine now the structure of this approximation scheme more closely. Substitution of Eq. (37) into Eq. (31) yields with $\vec{q} = (0, 0, q_3)$

$$N_L(q, z) = \frac{m\varphi_L^2(q)}{n^3} \sum_{\vec{k}, \vec{p}} \Psi_{\vec{k}\vec{p}}^{33}(q, z), \quad (38a)$$

$$N_T(q, z) = \frac{m\varphi_T^2(q)}{n^3} \sum_{\vec{k}, \vec{p}} [\Psi_{\vec{k}\vec{p}}^{11}(q, z) + \Psi_{\vec{k}\vec{p}}^{22}(q, z)] / 2. \quad (38b)$$

Introducing $\kappa = |\vec{q} - \vec{k}|$ as an integration variable one gets from Eq. (29)

The spectrum of the fluctuating forces $M''_{L,T}(q, \omega)$ determines the real part of the relaxation kernels $M'_{L,T}(q, \omega)$ by a Kramers-Kronig relation according to the Eq. (2),

$$M'_{L,T}(q, \omega) = P \int d(\epsilon/\pi) M''_{L,T}(q, \epsilon) / (\epsilon - \omega). \quad (41)$$

Equation (11) yields the spectrum for the trans-

verse modes,

$$\Phi''_T(q, \omega) = \frac{(n/m)M''_T(q, \omega)}{[\omega^2 - \Omega_T^2(q) + \omega M'_T(q, \omega)]^2 + [\omega M''_T(q, \omega)]^2}, \quad (42)$$

and from Eq. (15) the spectrum of the longitudinal excitations is found to be

$$\Phi''_L(q, \omega) = (n/m)M''_L(q, \omega) \left[\left(\omega^2 - \Omega_L^2(q) + \frac{[\omega^2 - \Omega_0^2(q)]M'_L(q, \omega)}{\omega} \right)^2 + \left(\frac{[\omega^2 - \Omega_0^2(q)]M''_L(q, \omega)}{\omega} \right)^2 \right]^{-1}. \quad (43)$$

If one considers besides the trivial parameters temperature T , particle density n , and particle mass m the frequency-independent functions $\Omega_{L,T}(q)$, $\Omega_0(q)$, and $\varphi_{L,T}(q)$ as given—they are all given by the known two-particle interaction and by the known pair-correlation function $g(r)$ —Eqs. (39)–(43) present a closed nonlinear system to determine the excitation spectrum. Notice that via Eqs. (39) and (40) the longitudinal excitations are coupled with the transverse ones. The preceding equations can be solved by iteration. The n th approximation $M^{(n)}_{L,T}(q, \omega)$ determines the n th approximation $\Phi^{(n)}_{L,T}(q, \omega)$ with the aid of Eqs. (41)–(43). Then Eqs. (39) and (40) yield the $(n+1)$ st approximation for the relaxation kernels.

We want to demonstrate the preceding approximation scheme for argon since the best experimental information about monatomic classical liquids is available for this fluid. We choose $T = 85^\circ \text{K}$, $n = 2.14 \times 10^{22} \text{ cm}^{-3}$, $m = 66.28 \times 10^{-24} \text{ g}$ and take the characteristic frequencies according to Eqs. (10b) and (14a) from the preceding literature.^{3, 4, 34} Together with the quantity $\Delta^2(q)$ from Eq. (14b) these frequencies are represented in Fig. 2 for the sake of completeness. Choosing in Eq. (36c) $r_0 = 3.4 \text{ \AA}$ and the Einstein frequency³⁵ $\Omega_E = 0.74 \times 10^{13} \text{ sec}^{-1}$ the frequencies $\Omega_{L,T}(q)$ are reproduced within 5%. Thus we used these parameters to work out the three-current vertex (37). The hard-core parameter has been chosen as $r_1 = 3.3 \text{ \AA}$ according to the experimental $g(r)$.³⁴ The result is plotted in Fig. 2. Hence all input quantities for the self-consistency equations are fixed.

If one assumes our system to have relatively well-defined excitation modes with dispersion curves similar to the ones shown in Fig. 2, the density of states for the current excitations will be divergent for momenta of the longitudinal modes close to 1 \AA^{-1} or 2 \AA^{-1} and for the transverse modes around 2 \AA^{-1} . Owing to this one expects then van Hove singularities in the spectra of the fluctuating forces $M''_{L,T}(q, \omega)$, which in turn yield a characteristic structure in the response function $\Phi''_{L,T}(q, \omega)$. This clearly comes out if one starts iterating the self-consistency equations by neglecting all damp-

ing effects in zeroth order: $M^{(0)}_{L,T}(q, z) = 0$. Actually, one can approximate then the integrals (39) and (40) for $M^{(1)}_{L,T}(q, \omega)$ in terms of elementary functions and some of those results are given in the Appendix. Originally we expected the final solutions of Eqs. (39)–(43) to show some structure similar to that of $M^{(1)}_{L,T}(q, \omega)$. For this reason we have started the iteration with $M^{(0)}_{L,T}(q, z) = 0$. Five iterations have been necessary to get the solutions stable within 10% and to learn that the excitation modes are too broad to yield much structure in $M''_{L,T}(q, \omega)$. So the most convenient starting point for the iteration would have been the ansatz $M^{(0)}_{L,T}(q, \omega) = -a/(\omega^2 + D^2)$, where D is of the order of the characteristic frequency $\Omega_{L,T}(q)$ and a is

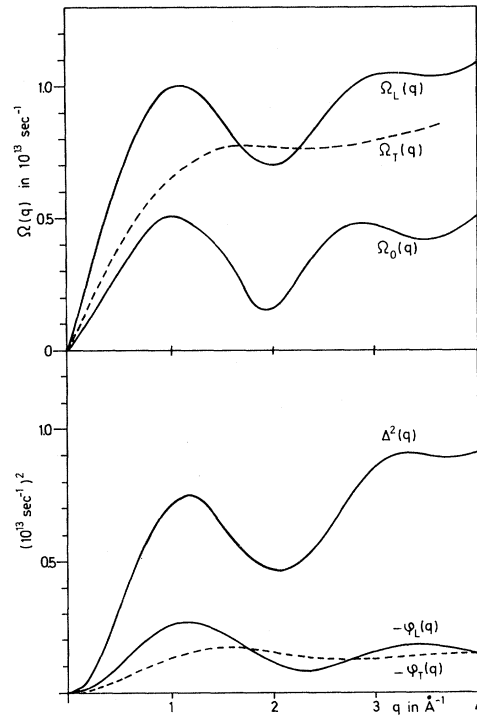


FIG. 2. Characteristic frequencies $\Omega_{L,T}(q)$, $\Omega_0(q)$, the quantity $\Delta^2(q) = \Omega_L^2(q) - \Omega_0^2(q)$, and the vertex functions $-\varphi_{L,T}(q)$ as a function of wave number for liquid argon.

chosen to get $M^{(0)} - M^{(1)}$ as small as possible. But using such an ansatz one would have lost some of the physical insight into the damping mechanism (cf. Appendix).

B. Correlation functions for liquid argon

In Figs. 3 and 4 the relaxation kernels $M_L''(q, \omega)$ and $M_T''(q, \omega)$ are shown in comparison with the memory kernels obtained by computer simulations. To get the latter curves we have taken Rahman's^{3,4} curves for $\Phi''(q, \omega)$, calculated by Kramers-Kronig analysis [see Eq. (2a)] $\Phi'(q, \omega)$, and then inverted Eqs. (11) and (15), respectively, to find $M(q, z)$. In principle the full curves of Figs. 3 and 4 are the known experimental kernels. It should be realized, however, that small errors in reading off $\Phi''(q, \omega)$ introduce big errors in $M''(q, \omega)$; the expression for M contains Φ'' and Φ' in differences of big numbers in the denominator for example. Also the Kramers-Kronig analysis transfers errors of Φ'' in one frequency range into errors of M'' in different frequency intervals. We can say that the kernels given as full curves in Figs. 3 and 4 reproduce Rahman's graphs^{3,4} of Φ'' within pencil width, but we also found that curves with artificial spikes did the same. The decrease of $M_L''(q, \omega)$ for small ω in the full curves of Fig. 3 is due to the wrong low-frequency behavior of Rahman's $\Phi_L''(q, \omega)$; it has no real physical meaning therefore. There is no pronounced difference between the longitudinal and transverse relaxation spectrum, but the latter function is somewhat smaller than the first one. Both kernels are rather smooth. They show a broad maximum at about $0.5 \times 10^{13} \text{ sec}^{-1}$ and they drop off quickly for frequencies larger than $2 \times 10^{13} \text{ sec}^{-1}$. Concerning these features there is qualitative agreement between our calculations and the experiment.

In Fig. 5 the longitudinal excitation spectra are shown in comparison with the neutron scattering data of Sköld *et al.*² and with the computer data of Rahman³ and Levesque *et al.*⁶ For the sake of comparison we interpolated some of the experimental data between different wave-number values. The excitation spectra show non-Lorentzian resonances whose peaks and widths are plotted as functions of the wave number in Fig. 6. The resonance width increases upon increasing the wave number from 0.5 towards 1 Å^{-1} . Then the resonance becomes sharper and a characteristic high-frequency shoulder appears for larger q values. For q beyond 2.5 Å^{-1} the peaks become broader again and there is no shoulder. All these facts are given by the present theory in good qualitative agreement with the experimental data.^{2,3,6} The peak height drops quickly if q increases from 0.5 towards

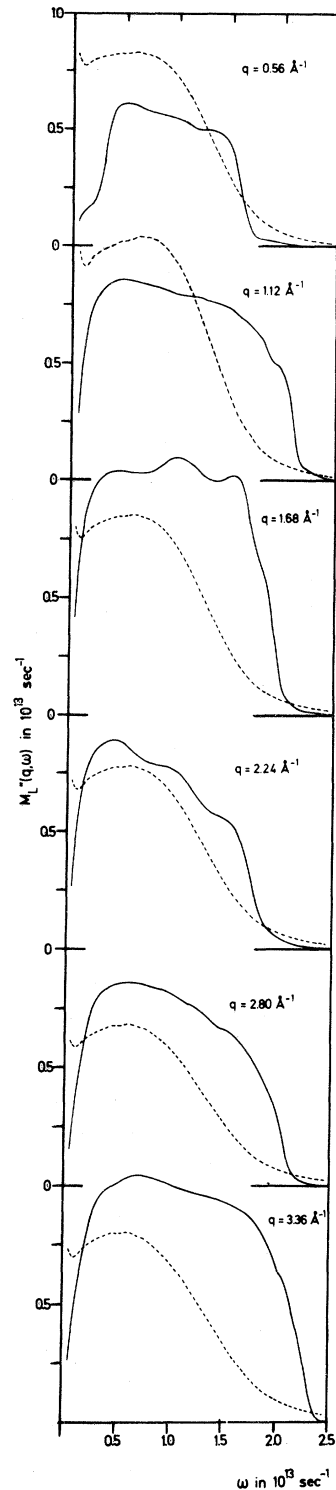


FIG. 3. Longitudinal relaxation kernels $M_L''(q, \omega)$. The full curves are extracted from Rahman's computer experiments (Ref. 3); the dashed curves are the results of the present theory.

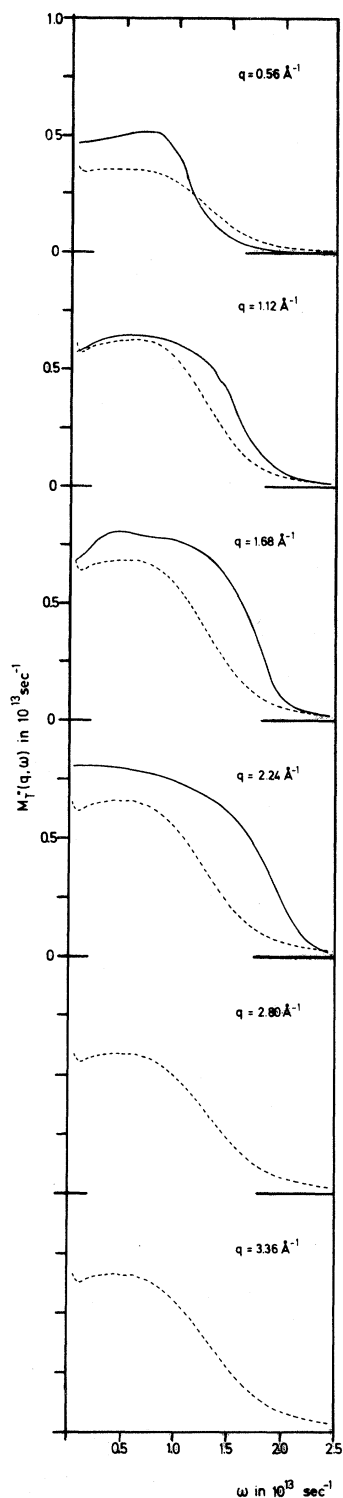


FIG. 4. Transverse relaxation kernels $M_T''(q, \omega)$. The full curves are extracted from Rahman's computer experiments (Refs. 3 and 4); the dashed curves are the results of the present theory.

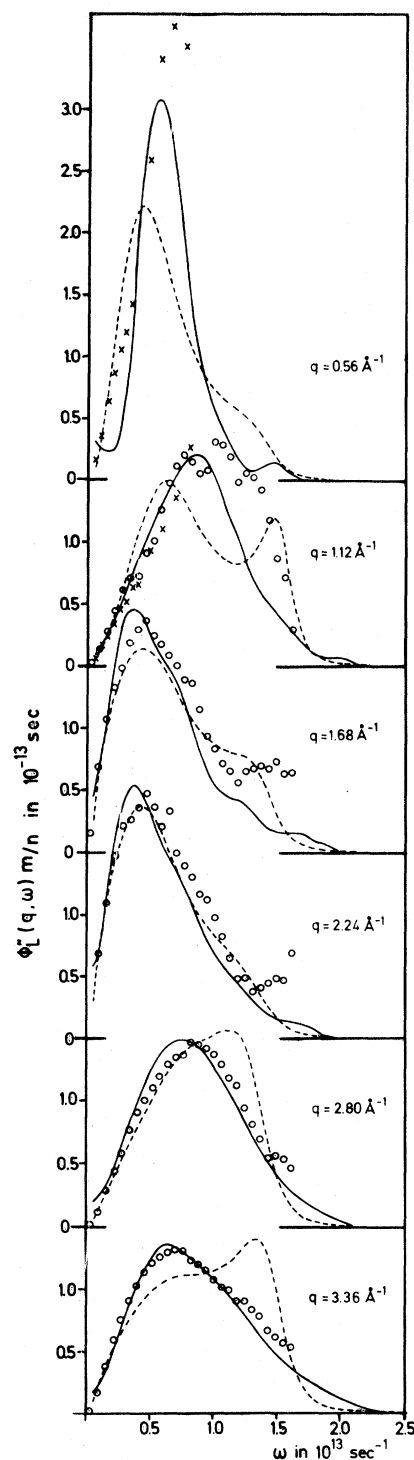


FIG. 5. Longitudinal excitation spectra $\Phi_L''(q, \omega)m/n$ as a function of frequency for various wave numbers. The full curves are the result of Rahman's computer experiments (Ref. 3), crosses denote computer data of Levesque *et al.* (Ref. 6), and the circles are neutron scattering data of Sköld *et al.* (Ref. 2). The dashed curves are the results of the present theory.

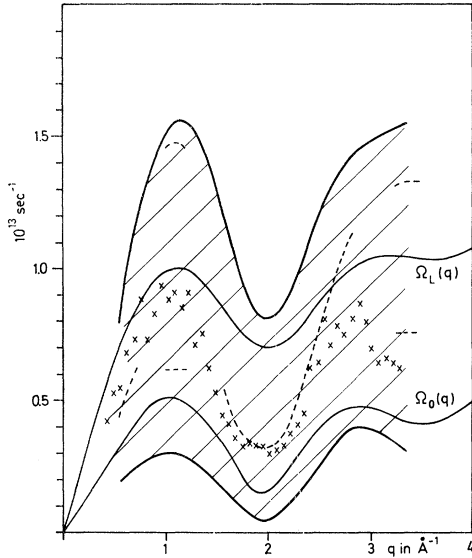


FIG. 6. Peak positions of the longitudinal current excitations (dashed curve) and half-width (thick curves) as a function of wave number. The crosses are Rahman's data (Ref. 3) for the peak positions. Included are the frequencies $\Omega_L(q)$ and $\Omega_0(q)$ (thin curves).

1 \AA^{-1} ; then it increases for q towards 2 \AA^{-1} and it drops slowly if q increases beyond 2.5 \AA^{-1} . These facts are given by the present theory in qualitative agreement with the experimental data; but for q smaller than 1.2 \AA^{-1} excitation states are missing in our $\Phi_L''(q, \omega)$. Owing to this defect we erroneously even get for $q \sim 1 \text{ \AA}^{-1}$ a double-peak structure. The peak position is close to $\Omega_0(q)$ for $q \sim 2 \text{ \AA}^{-1}$ and it moves towards $\Omega_L(q)$ for other wave numbers. This feature is reflected by the present theory but for a q larger than 3 \AA^{-1} our peak positions are too high. Since $\Phi_{\rho\rho}''(q, \omega)$ directly gives the coherent-inelastic-neutron-scattering cross section, $S(q, \omega)$ is plotted in Fig. 7 together with various experimental data. The neutron cross section is a non-Lorentzian peak centered at $\omega=0$ showing a characteristic variation of its width as a function of wave number. Most of the detailed structure of $\Phi_L''(q, \omega)$ is washed out in the $S(q, \omega)$ curves and this explains the quantitative agreement of our theoretical results with the experimental ones.

In Fig. 8 the transverse excitation spectra are plotted. One obtains resonances close to the characteristic frequency $\Omega_T(q)$ which are still present for q as small as 0.5 \AA^{-1} . Their width increases with increasing wave number; this behavior is also represented in Fig. 9. For q values exceeding 1.5 \AA^{-1} the resonance curves are rather non-Lorentzian. Particularly interesting is the sharp drop of $\Phi_T''(q, \omega)$ for frequencies approaching $1.4 \times 10^{13} \text{ sec}^{-1}$. There is satisfactory agreement

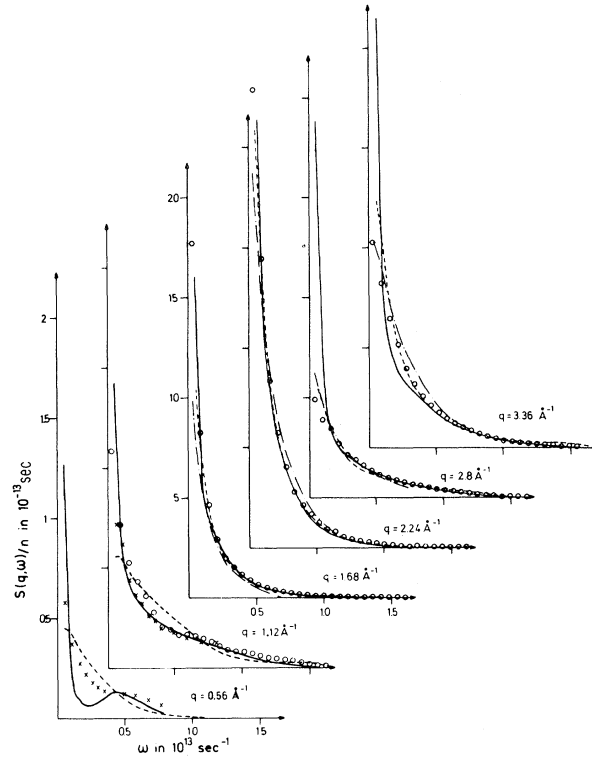


FIG. 7. Coherent-scattering function $S(q, \omega)/n$ (dashed curves) as a function of frequency for various wave numbers. The circles are the neutron scattering data by Sköld *et al.* (Ref. 2). The full curves are the results of the computer experiment by Rahman (Ref. 3), the dashed dotted the ones by Kurkijärvi (Ref. 5), and the crosses the ones by Levesque *et al.* (Ref. 6). Notice the different ordinate scale for the two lowest wave vectors. In particular for $q=2.24$ the present results cannot be distinguished from Rahman's.

between our theoretical curves and the computer experiments.^{3, 4, 6}

IV. DISCUSSION

The preceding theory for the excitation spectrum of liquids is based on the exact representations [Eqs. (11) and (15)] of the current-current relaxation functions in terms of the well-known characteristic frequencies $\Omega_T(q)$, $\Omega_L(q)$, and $\Omega_0(q)$ and of relaxation kernels $M_T(q, z)$ and $M_L(q, z)$. The latter quantities contain all the nontrivial dynamics of the many-particle system. Their absorptive parts $M_{T, L}''(q, \omega)$ can be interpreted as spectra of the fluctuating forces disturbing the secular motion characterized by the frequencies $\Omega_L(q)$, $\Omega_T(q)$, and $\Omega_0(q)$. These spectra have been approximated by a Golden Rule type of formula [Eqs. (29) and (31)] expressing the decay of a coherent current excitation into pairs of such modes. The three-current decay vertex (see Fig. 1) entering the ex-

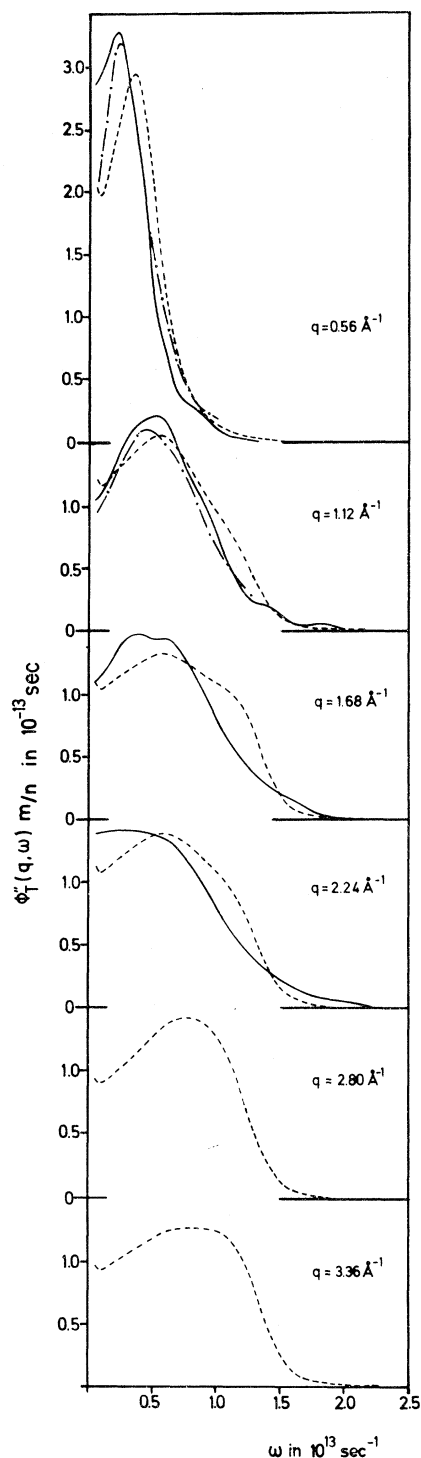


FIG. 8. Transverse excitation spectra $\Phi_T''(q, \omega)m/n$ as a function of frequency for various wave numbers. The full curves and the dashed dotted ones are the results of the computer experiments by Rahman (Refs. 3 and 4) and Levesque *et al.* (Ref. 6), respectively.

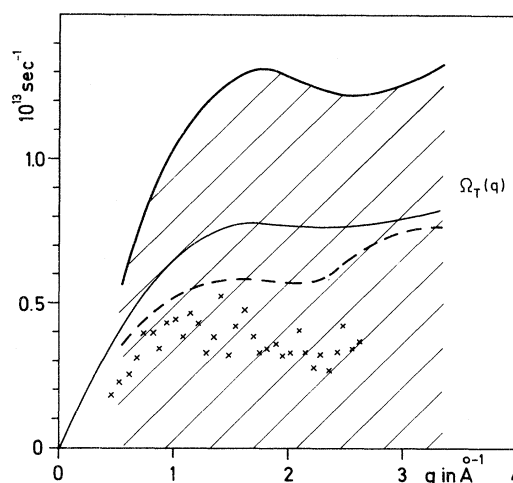


FIG. 9. Transverse resonance position (dashed curve) and width (full curve) as a function of wave number. The crosses are Rahman's data (Ref. 3) for the peak positions. The thin curve represents $\Omega_T(q)$.

pressions for $M_{L,T}''(q, \omega)$ was given by the irreducible part of a three-particle correlation function. The latter was evaluated approximately by taking into account three-particle hard-core correlations; see Eqs. (34) and (35). Then a closed set of coupled self-consistency equations, Eqs. (39)–(43), appeared expressing the relaxation kernels in terms of the current excitation spectra. The solution of these equations are obtained by iteration, but the main features of the excitation spectra obtained can be understood without going into numerical details.

The characteristic frequencies $\Omega_{L,T}(q)$ and $\Omega_0(q)$ for wave numbers corresponding to the main particle distance are of the same order, $0.7 \times 10^{13} \text{ sec}^{-1}$, as the typical Einstein frequency Ω_E , where $\Omega_E^2 = (n/3m) \int dr g(r) \Delta v(r)$. It has been shown that the characteristic energy $|\varphi_{L,T}(q)|^{1/2}$ (see Fig. 2) describing the three-current decay is also of this order of magnitude. At the temperature of liquid argon there is essentially only one energy scale in the system as far as the regime of intermediate values of frequencies ω and wave numbers q is concerned. This first crucial point came out by carefully examining the three-particle correlations. Erroneously misestimating φ by a factor of 4, say, in either direction would change completely the following discussion and bring out quite a wrong picture for the excitation spectra. From this estimation one gets the second conclusion: The relevant absorption parts $M_L''(q, \omega)$ and $M_T''(q, \omega)$ are also of the order of magnitude of Ω_E and hence the widths of the typical excitations are of the same order as their energies; consequently there is no fine structure in the fluctuation spectra $M_{L,T}''(q, \omega)$.

In zeroth approximation the current excitations are modes with dispersion $\Omega_L, \tau(q)$. Thus for a decay process with a transverse mode in the final state one expects a huge phase space for the energy of this mode being around the plateau value $0.7 \times 10^{13} \text{ sec}^{-1}$ (see Fig. 2). The phase space is also large if the final longitudinal mode corresponds to the maximum near $q \sim 1 \text{ \AA}^{-1}$ or to the minimum near $q \sim 2 \text{ \AA}^{-1}$ of the $\Omega_L(q)$ dispersion curve; but these enhancements correspond to a small domain in q space only and are by far not so important as the corresponding enhancements of the transverse modes. Furthermore there are twice as many transverse modes than longitudinal ones. Thus we arrive at the third important fact: Decay processes with a transverse excitation involved are more important than decay processes where only longitudinal modes interact; i.e., coupling to the transverse modes is crucial for analyzing the longitudinal excitation spectrum $\Phi_L''(q, \omega)$. Quantitatively it turned out that decay processes involving a transverse mode contribute, e.g., to $M_L''(q, \omega)$ roughly twice as much as those processes involving longitudinal modes only. For kinematical reasons those processes involving a transverse mode contribute most effectively for $\omega \sim \Omega_E$. So one concludes fourthly that the relaxation spectra $M_{L, \tau}''(q, \omega)$ as a function of frequency show some bump for intermediate ω . Fifth, for frequencies of order $2\Omega_E$ the fluctuation spectra drop quickly since higher states cannot be reached by two mode processes. Sixth, for frequencies below Ω_E the spectra $M_{L, \tau}''(q, \omega)$ are rather flat since many processes contribute: In classical systems the difference process, where e.g., a longitudinal mode absorbing a longitudinal excitation combines to a transverse one, is as important as the sum process, where the longitudinal mode decays into a transverse plus a longitudinal excitation.

The relaxation spectra directly determine now the current-current relaxation functions. Since $[\varphi_T(q)/\Omega_T(q)]^2$ vanishes for vanishing q and since for small q the conservation laws drastically restrict the phase space for two mode processes one concludes seventh that for wave numbers smaller than 0.5 \AA^{-1} there is still a well-defined transverse current excitation resonance.⁶ These excitations could be called transverse zeroth sound. Eighth, for q 's exceeding 1.5 \AA^{-1} the transverse resonances have an almost q -independent position; the resonance curve $\Phi_T''(q, \omega)$ is rather flat on the low-frequency side and drops steeply for frequencies approaching $2\Omega_E$.

The structure of (15) and (43) for the longitudinal excitation is more interesting than the one of the transverse response function. To understand the

interplay of the two frequencies $\Omega_L(q)$ and $\Omega_0(q)$ let us consider two limiting cases. If $M_L(q, z)$ is small there is a longitudinal resonance with frequency $\Omega_L(q)$ and width $M_L''(q, \Omega_L(q))$. If $M_L(q, z)$ is large there is a resonance at $\Omega_0(q)$ having the width $\sim \Delta^2(q)/M_L''(q, \Omega_0(q))$. In the first case one has the situation of slow relaxation while in the second case the fast relaxation yields the effect of motional narrowing: The random forces fluctuate so fast that essentially only the average is seen in the response. According to our first point in the preceding discussion the magnitude of $M_L(q, \omega)$ for intermediate q is such that neither limiting case occurs. One concludes that the vanishing of the long-wavelength vertex, ninth, brings the system towards the slow relaxation limit for q smaller than 0.5 \AA^{-1} . Similar to the situation in the transverse case the longitudinal response function exhibits a rather narrow zero-sound resonance.

With increasing momentum the resonance becomes broader. Tenth, for a q around 1.7 \AA^{-1} , $\Delta^2(q)$ gets small enough and the decay channels are open most efficiently to drive the system closer to the fast-relaxation limit. The resonance position moves away from $\Omega_L(q)$ towards $\Omega_0(q)$, the peaks becoming sharper. Of course, M'' is not really very large and, therefore, eleventh, the resonance $\Omega_L(q)$ shows up in the spectrum as a high-frequency shoulder. It is situated considerably above $\Omega_L(q)$ because the real part $M_L'(q, \omega)$ of the relaxation kernel re-normalizes this second resonance. For wave numbers larger than 2 \AA^{-1} , twelfth, $\Delta^2(q)$ increases and so the system gradually draws back to the regime of slower relaxation. Hence for larger q 's the resonance becomes broader and the position moves towards $\Omega_L(q)$. The characteristic oscillation of the resonance width as a function of wave number—see Fig. 6—thus are a direct consequence of the two-mode decay kinematics and the behavior of $\Delta^2(q)$.

Figures 4–9 demonstrate satisfactory quantitative agreement of the present theory with the experimental data as far as the neutron cross section and the transverse excitation spectrum is concerned. For the more detailed information expressed by the longitudinal current excitation spectrum good agreement with experiments has been achieved for wave numbers around the roton minimum. For larger q 's and for small q 's the agreement with the experiment is not so good; for $q \sim 1 \text{ \AA}^{-1}$, i.e., near the boundary of the Brillouin zone of the solid argon system, excitation states are missing in $\Phi_L''(q, \omega)$. Systematic errors become obvious for q tending towards 0.5 \AA^{-1} and q exceeding 3.3 \AA^{-1} .

The most annoying errors of the present theory are the discrepancies between the theoretical and experimental $\phi_L''(q, \omega)$ for wave numbers around and below 1 \AA^{-1} . One realizes from Fig. 3 that this error is due to our M_L'' being too large compared with the Rahman data. Possibly this error is due to our neglect of the energy-density mode which couples to Φ_L but not to Φ_T . Another source of error is our rough handling of the vertex $\varphi(\vec{q}, \vec{k})$ by dropping its \vec{k} dependence. For $q \rightarrow 0$ it is also not allowed to neglect the contribution (33e). This term actually yields the hydrodynamical $D(0, 0)$ and $\Gamma(0, 0)$ in Eqs. (16). For anharmonic lattices the hydrodynamical limit has been analyzed within the Mori formalism³⁶; there it has been found that three excitation decay processes determine the transport coefficients. So it seems likely that these processes are important in the hydrodynamical limit of liquids also. It is feasible to take care of the points mentioned, but because of the work required we have not yet analyzed the $q \rightarrow 0$ limit quantitatively.

It is understandable that our memory kernels $M''(q, \omega)$ in general are smaller than the experimental ones, since the two-mode approximation neglects excitations of a different type. Since our approximation excludes the free-gas limit, this error becomes more important with larger q . One can incorporate the free-gas limit by adding in lowest order the free-gas memory kernel to the one calculated above. This improves the theory for large q , but there are still systematic deviations from experiment, indicating that the large- q discrepancies have a less trivial reason.

In this paper we wanted to show that a first-principles theory for classical liquids can be tried and that a lowest-order approximation can be carried out to an end. We consider it encouraging that the results in some aspects come close to experiment. Therefore it might be worthwhile to work out quantitative improvements of the approach presented above.

ACKNOWLEDGMENTS

We thank Dr. H.-J. Schirlitzki and Dr. P. Wölfle for helpful discussions.

APPENDIX: DECAY KINEMATICS AND THE RELAXATION KERNELS $M_{L,T}(q, z)$ FOR DIFFERENT ITERATION STEPS

We started our iterative procedure for solving Eqs. (39)–(43) by the ansatz $M_{L,T}(q, z) = 0$, i.e., by assuming undamped modes. Then $M^{(1)}(q, \omega)$ has the structure of the density of states for non-interacting, undamped two-mode excitations,

$$M^{(1)}(q, \omega) = \int_0^\infty dk \int_{|q-k|}^{q+k} d\kappa \delta(\omega \pm \Omega_{L,T}(\kappa) \pm \Omega_L(k)) \times f(q, k; \kappa), \quad (\text{A1})$$

where $f(q, k; \kappa)$ abbreviates geometry factors according to Eqs. (39) and (40). A summation over all possible sign combinations in the δ function corresponding to different decay processes has to be included. The κ integration in (A1) yields

$$M^{(1)}(q, \omega) = \sum_n \int_{\mathfrak{D}_n} dk \left| \frac{\partial \Omega_{L,T}(\kappa)}{\partial \kappa} \right|_{\kappa=\kappa_n}^{-1} \times f(q, k; \kappa_n), \quad (\text{A2})$$

where n counts the energy conserving solutions $\kappa_n = \kappa_n(\omega, k)$ of $\omega \pm \Omega_{L,T}(\kappa) \pm \Omega_L(k) = 0$. The k integration is extended over that fraction $\mathfrak{D}_n(q, \omega; k)$ of k space $|q - k| \leq \kappa_n(\omega, k) \leq q + k$ which guarantees momentum conservation. From Eq. (A2) one immediately concludes that $M^{(1)}(q, \omega)$ will have van Hove singularities due to the possible zeros of $\partial \Omega_{L,T}(\kappa)/\partial \kappa$; see Fig. 2. Furthermore it is clear that decays involving a transverse mode contribute most. So we restricted ourselves in the first iteration step to the LT-type decay processes, as shown in Fig. 10, involving a transverse mode. For all further iteration steps the corresponding LL processes are taken into account.

In order to find closed expressions for the hyperplane $\mathfrak{D}_n(q, \omega; k)$ upon which energy and momentum conservation allow decays we approximated $\Omega_{L,T}(q)$ for this first iteration step by

$$\Omega_L(q) \approx \omega_0 \omega_L(\hat{q}) = \omega_0 \begin{cases} \hat{q}(2 - \hat{q}) & \text{for } \hat{q} \leq \frac{5}{4} \\ \frac{3}{4} + (\hat{q} - 2)^2/3 & \text{for } \hat{q} \geq \frac{5}{4} \end{cases}, \quad (\text{A3a})$$

$$\Omega_T(q) \approx \omega_0 \omega_T(\hat{q}) = \omega_0 \begin{cases} \hat{q}(4 - \hat{q})/5 & \text{for } \hat{q} \leq 2 \\ \frac{4}{5} & \text{for } \hat{q} \geq 2 \end{cases}, \quad (\text{A3b})$$

with $\hat{q} = q/Q_0$, $Q_0 = 1.12 \text{ \AA}^{-1}$, and $\omega_0 = \Omega_L(Q_0) = 10^{13} \text{ sec}^{-1}$.

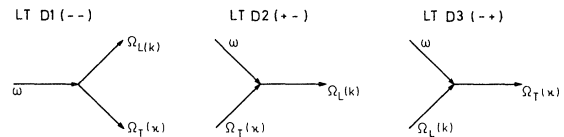


FIG. 10. LT-type decay processes contributing to Eq. (A1). The process corresponding to the sign combination $(++)$ contributes only for negative frequencies.

In the following we will omit the carets characterizing reduced units. Using Eq. (A3) the two-mode singularities of $M^{(1)}(q, \omega)$ can be localized without going too much into numerical details.

$$M^{(1)}(q, \omega)|_{\kappa \geq 2} = \int_0^\infty dk \delta(\omega \pm \frac{4}{5} \pm \omega_L(k)) \int_{\max(2, |q-k|)}^{q+k} dk f(q, k; \kappa) = \sum_n \left| \frac{\partial \omega_L(k)}{\partial k} \right|^{-1} \int_{k=k_n}^{q+k_n} dk f(q, k_n; \kappa).$$

(A4)

This yields singularities in the (ω, q) plane for those (ω, q) values which allow both decay partners to reach divergent final-state densities as shown in Fig. 11. In other words: To produce two-mode singularities both single modes must come from regions with vanishing derivatives of the dispersion curve. Let us demonstrate this for the decay LTD1 defined by the solutions of energy conservation $\omega - \frac{4}{5} - \omega_L(k) = 0$:

$$k_{A,B} = 1 \mp (\frac{9}{5} - \omega)^{1/2}, \quad k_{C,D} = 2 \mp (\omega - \frac{31}{20})^{1/2}. \quad (\text{A5a})$$

The index A, B, \dots refers to different regions of the longitudinal dispersion as marked in Fig. 11. Then

$$\left| \frac{\partial \omega_L(k)}{\partial k} \right|_{k=k_n} = \begin{cases} 2(\frac{9}{5} - \omega)^{1/2}, & A, B \text{ solution } k \leq \frac{5}{4} \\ \frac{2}{3}\sqrt{3}(\omega - \frac{31}{20})^{1/2}, & C, D \text{ solution } k \geq \frac{5}{4} \end{cases} \quad (\text{A5b})$$

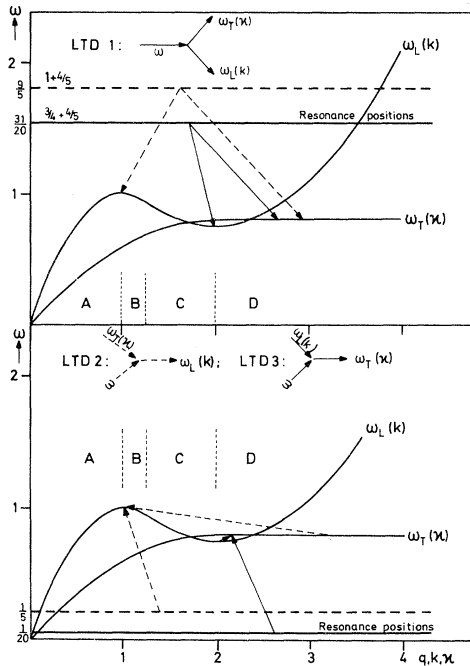


FIG. 11. Positions of two-mode resonance in the (ω, q) plane caused by different LT-type decay processes.

The dominant contribution to the integral (A2) comes from $\kappa \geq 2$, i.e., from the flat part of $\omega_T(\kappa)$. Let us discuss these contributions to $M^{(1)}(q, \omega)$ first:

Thus the decay LTD1 will lead to a square-root singularity in $M^{(1)}(q, \omega)$ at $\omega = \frac{31}{20}$ for all q which fulfill momentum conservation together with $k=2$. A second singularity at $\omega = \frac{9}{5}$ involves the longitudinal excitation with wave number $k=1$. Both resonance positions in the (ω, q) plane being determined by Eq. (A5) and momentum conservation are shown in Fig. 11. Similarly one finds the decay processes LTD2, 3 to cause singularities in Eq. (A4) for frequencies $\omega = \frac{1}{5}$ and $\omega = \frac{1}{20}$, respectively as shown in Fig. 11. Qualitatively the four singularities caused by LT-type decay processes are equally strong. But if one takes into account the function $f(q, k_n; \kappa)$ in (A4) one finds that the singularities formed with the longitudinal mode from the dip of the dispersion at $k=2$ are stronger than those formed with $\omega_L(k)$ originating from the maximum at $k=1$. This causes the singularities at frequencies $\omega = \frac{9}{5}$ and $\omega = \frac{1}{5}$ to be much less pronounced than those at $\omega = \frac{31}{20}$ and $\omega = \frac{1}{20}$, respectively.

After having located the positions of two-mode singularities in the ω - q plane let us investigate the hyperplanes $\mathfrak{D}_n(q, \omega; k)$ upon which LT decays are allowed. For the special case involving transverse excitations with wave numbers $\kappa \geq 2$ one merely has to look for those (ω, q) values which fulfill

$$\max(2, |k_n(\omega) - q|) \leq k_n(\omega) + q, \quad (\text{A6})$$

where $k_n(\omega)$ are the solutions of energy conservation $\omega \pm \frac{4}{5} \pm \omega_L(k) = 0$. Thus one has to make for each of the three different decay processes LTD1, 2, 3 four separate investigations to determine for which (ω, q) values the four solutions of energy conservation obey Eq. (A6).

To evaluate the hyperplanes for LT decays involving transverse excitations with wave numbers $\kappa \leq 2$ is a bit more tedious. We will indicate the procedure for the LTD1 process: $\omega - \omega_T(\kappa) - \omega_L(k) = 0$. With the constraint $\kappa \leq 2$ there is only one solution of energy conservation,

$$\kappa_1(\omega, k) = 2 - \{4 - 5[\omega - \omega_L(k)]\}^{1/2}. \quad (\text{A7})$$

Then the inequalities

$$|k - q| \leq \kappa_1(\omega, k) \leq k + q \quad (\text{A8a})$$

define the hyperplane $\mathfrak{D}_1(q, \omega; k)$ for the decay LTD1. Since $\omega_T(q)$ is a monotonic function, (A8a) reads also

$$\omega_T(|k - q|) \leq \omega - \omega_L(k) \leq \omega_T(k + q). \quad (\text{A8b})$$

The latter form of the inequality can better be represented graphically and it contains naturally the constraint $\kappa \leq 2$ as well as energy conservation. With the aid of a graphical representation of Eq. (A8b) we analytically determined the range of k values fulfilling Eq. (A8b) as a function of frequency for fixed wave numbers q .

Figure 12 shows the contributions of all LT decay processes to the longitudinal relaxation kernel $N_L^{(1)}(q = \frac{3}{2}, \omega)$ as a representative example. There are sharp two-mode singularities as discussed before at frequencies $\omega = \frac{1}{20}$ and $\omega = \frac{31}{20}$ above a flat continuum. The intensity of the singularities at frequencies $\omega = \frac{1}{5}$ and $\omega = \frac{2}{5}$ is so small that one cannot recognize them on the scale of Fig. 12. The finite kernel $M^{(1)}(q, \omega)$ causes broadened resonances of the current relaxations $\Phi^{(1)}(q, \omega)$, which in turn lead via the convolution integrals (39) and (40) to a bigger continuum in $M^{(2)}(q, \omega)$ with broader two-mode resonances than in $M^{(1)}(q, \omega)$. The contribution to the relaxation spectrum $M_L^{(2)}(q, \omega)$ of the second iteration from LL processes is roughly half as big as that one from LT decays. The double peak in $M_L^{(2)}(q, \omega)$ at frequencies $\omega \approx 0.8 \pm 0.06$ and $\omega \approx 0.8 - 0.06$ is caused by LTD1 and LTD3 processes, respectively, involving a transverse mode from the flat part of the dispersion of $\Phi_T^{(1)}$ at $\omega \approx 0.8$ and a longitudinal excitation from the dip at $k = 2$ with frequency $\omega \approx 0.06$. [Note that $\Phi_L^{(1)}(q, \omega)/\omega^2$ enters the convolution integral (39) for $M^{(2)}$, and $\Phi_L^{(1)}(q, \omega)/\omega^2$ exhibits for $q = 2$ a strong hybridization peak at $\omega \approx 0.06$ caused by the singularity of $M^{(1)}(q, \omega)$ at $\omega = \frac{1}{20}$.] Similarly the other peaks of $M^{(2)}(q, \omega)$ can be identified by specific decays.

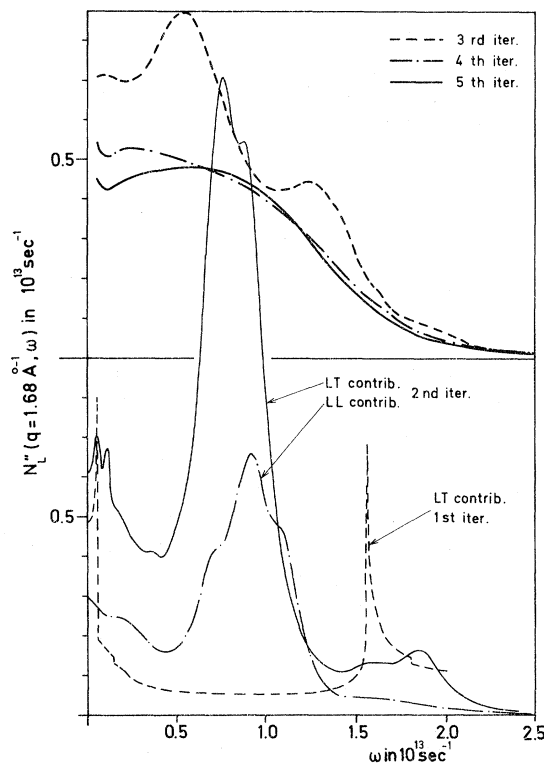


FIG. 12. Longitudinal relaxation kernels $N_L^{(1)}(q, \omega)$ of five iteration steps as a function of frequency ω for the representative wave number $q = 1.68 \text{ \AA}^{-1}$. For the second iteration the contributions from LT-type processes are displayed separately.

The main structure of the relaxation spectra $M^{(n)}(q, \omega)$ for further iteration steps is caused again by LT contributions involving transverse excitations from the flat part of the dispersion, i.e., with frequency $\omega \approx 0.8$ and longitudinal excitations from the dip with wave number $q = 2$. Since $\Phi_L^{(n)}(q, \omega)/\omega^2$ has its main peak for higher iteration steps at zero frequency this explains the surviving of the broad maximum at $\omega \approx 0.8$ in the kernel $M^{(n)}(q, \omega)$ as a result of LT-type processes.

- ¹N. Kroo, G. Borgonovi, and K. Sköld, Phys. Rev. Lett. **12**, 721 (1964); S. H. Chen, O. J. Eder, P. A. Egelstaff, B. C. G. Haywood, and F. J. Webb, Phys. Lett. **19**, 269 (1965); B. A. Dasannacharya and K. R. Rao, Phys. Rev. **137**, A417 (1965); K. Sköld, and K. E. Larsson, Phys. Rev. **161**, 102 (1967); K. E. Larsson, in *Neutron Inelastic Scattering* (International Atomic Energy Agency, Vienna, 1968), Vol. I, p. 397.
- ²K. Sköld, J. M. Rowe, G. Ostrowski, and P. D. Randolph, Phys. Rev. A **6**, 1107 (1972).
- ³A. Rahman, Phys. Rev. Lett. **19**, 420 (1967); in *Neutron Inelastic Scattering* (International Atomic Energy Agency, Vienna, 1968), Vol. I, p. 561.
- ⁴N. K. Ailawadi, A. Rahman, and R. Zwanzig, Phys.

- Rev. A **4**, 1616 (1971).
- ⁵J. Kurkijärvi, Ann. Acad. Sci. Fenn. A **VI346**, 1 (1970).
- ⁶D. Levesque, L. Verlet, and J. Kurkijärvi, Phys. Rev. A **7**, 1690 (1973).
- ⁷L. van Hove, Phys. Rev. **95**, 249 (1954).
- ⁸The well-known general formulas of linear response theory used in this paragraph can be found, e.g., in the lecture notes of P. C. Martin, Ref. 10.
- ⁹H. S. Wall, *Analytic Theory of Continued Fractions* (Van Nostrand, New York, 1948).
- ¹⁰P. C. Martin, *Problème à N corps*, edited by C. de Witt and R. Balian (Gordon and Breach, New York, 1968).
- ¹¹The longitudinal part of (10) was obtained classically

- by G. Placzek, Phys. Rev. 86, 377 (1952), and by P. G. de Gennes, Physica 25, 825 (1959). The transverse part is obtained as a corollary.
- ¹²R. Zwanzig and R. D. Mountain, J. Chem. Phys. 43, 4464 (1965).
- ¹³P. Schofield, Proc. Phys. Soc. Lond. 88, 149 (1966).
- ¹⁴R. Nossal and R. Zwanzig, Phys. Rev. 157, 120 (1967); 166, 81 (1968).
- ¹⁵M. Nelkin and S. Ranganathan, Phys. Rev. 164, 222 (1967); M. Nelkin and P. Ortoleva, in *Neutron Inelastic Scattering* (International Atomic Energy Agency, Vienna, 1968), Vol. I, p. 535.
- ¹⁶W. C. Kerr, Phys. Rev. 174, 316 (1968).
- ¹⁷K. S. Singwi, K. Sköld, and M. P. Tosi, Phys. Rev. Lett. 21, 881 (1968); Phys. Rev. A 1, 454 (1970); K. N. Pathak and K. S. Singwi, Phys. Rev. A 2, 2427 (1970).
- ¹⁸A. A. Kugler, J. Stat. Phys. 8, 107 (1973).
- ¹⁹J. Hubbard and J. L. Beeby, J. Phys. C 2, 556 (1969).
- ²⁰L. P. Kadanoff and P. C. Martin, Ann. Phys. (N.Y.) 24, 419 (1963).
- ²¹S. W. Lovesey, J. Phys. C 4, 3057 (1971); L. Bonamy and N. M. Hoang, Chem. Phys. Lett. 21, 470 (1973).
- ²²C. H. Chung and S. Yip, Phys. Rev. 182, 323 (1969).
- ²³H. Mori, Prog. Theor. Phys. 33, 423 (1965); 34, 399 (1965).
- ²⁴R. Zwanzig, in *Lectures in Theoretical Physics*, edited by W. Brittin and L. Dunham (Wiley-Interscience, New York, 1961), Vol. 3, p. 135.
- ²⁵P. Ortoleva and M. Nelkin, Phys. Rev. A 2, 187 (1970); F. Lado, Phys. Rev. A 2, 1467 (1970); 5, 2238 (1972); M. Hassan and F. Lado, J. Chem. Phys. 57, 3003 (1972); C. Murase, J. Phys. Soc. Jpn. 29, 549 (1970); 32, 1205 (1972); A. Z. Akcasu and E. J. Linnebur, in *Neutron Inelastic Scattering* (International Atomic Energy Agency, Vienna, 1972), p. 365.
- ²⁶V. F. Sears, Can. J. Phys. 48, 616 (1970); A. Z. Akcasu and E. Daniels, Phys. Rev. A 2, 962 (1970); K. Kim and M. Nelkin, Phys. Rev. A 4, 2065 (1971).
- ²⁷For a critical summary compare J. Rowe and K. Sköld, in *Neutron Inelastic Scattering* (International Atomic Energy Agency, Vienna, 1972), p. 413.
- ²⁸J. L. Lebowitz, J. K. Percus, and J. Sykes, Phys. Rev. 188, 487 (1969); D. Forster and P. C. Martin, Phys. Rev. A 2, 1575 (1970); D. Forster, Phys. Rev. A 9, 943 (1974).
- ²⁹G. F. Mazenko, Phys. Rev. A 3, 2121 (1970); 5, 2545 (1972); 9, 360 (1974); A. Z. Akcasu, Phys. Rev. A 7, 182 (1973).
- ³⁰J. J. Duderstadt and A. Z. Akcasu, Phys. Rev. A 1, 905 (1970); M. S. Jhon and D. Forster, Phys. Rev. A, (to be published).
- ³¹K. Kawasaki, Phys. Rev. 150, 291 (1966); Ann. Phys. (N.Y.) 61, 1 (1970); L. P. Kadanoff and J. Swift, Phys. Rev. 166, 89 (1968); F. Wegner, Z. Phys. 216, 433 (1968).
- ³²K. Kawasaki, Phys. Lett. 32A, 379 (1970); 34A, 12 (1971); R. Zwanzig, in *Proceedings of the Sixth IUPAP Conference on Statistical Mechanics*, edited by S. A. Rice, K. F. Freed, and J. C. Light (Univ. of Chicago Press, Chicago, 1972); T. Keyes and I. Oppenheim, Phys. Rev. A 7, 1384 (1973); P. Resibois, in *Irreversibility in the Many Body Problem*, edited by J. Biel and J. Rae (Plenum, New York, 1972).
- ³³See, e.g., J. A. Reissland, *The Physics of Phonons* (Wiley, London, 1973).
- ³⁴J. L. Yarnell, M. J. Katz, R. G. Wenzel, and S. H. König, Phys. Rev. A 7, 2130 (1973).
- ³⁵B. J. Berne, J. P. Boon, and S. A. Rice, J. Chem. Phys. 47, 2283 (1967).
- ³⁶W. Götze and K. H. Michel, in *Dynamical Properties of Solids*, edited by G. K. Horton and A. A. Maradudin (North-Holland, Amsterdam, 1974), p. 501.